Supporting information

Enhanced chemiresistive sensing performance of well-defined porous CuO-doped ZnO nanobelts toward VOCs

Gang Li,[†,‡,‖] Yao Su,[‡,‖] Xu-Xiu Chen,[†] Li Chen,[†,*] Yong-Yu Li,[†,‡] Zheng Guo[†,‡,*]

[†]Institute of Physical Science and Information Technology, Anhui University, Hefei 230601, People's Republic of China

Key Laboratory of Structure and Functional Regulation of Hybrid Materials, Anhui University, Ministry of Education, Hefei, 230601, People's Republic of China

[‡]Key Laboratory of Environmental Optics and Technology, Institute of Intelligent Machines, Chinese Academy of Sciences, Hefei 230031, People's Republic of China

*Correspondence should be addressed to L. Chen and Z. Guo.

E-mail: lichen@ahu.edu.cn (L. Chen), zhguo@iim.ac.cn (Z. Guo)

Tel.: +86-551-65595607; fax: +86-551-65592420.

‖G. Li and Y. Su contributed equally to this work.

Table of Contents

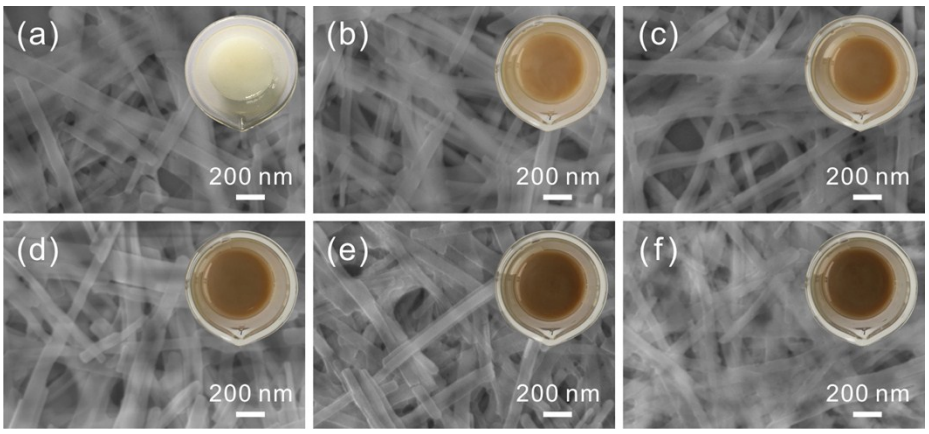

Figure S1. SEM images of $ZnSe{\cdot}0.5N_2H_4$ precursor nanobelts exchanged with different amount of Cu^{2+} cations: (a) pristine $ZnSe{\cdot}0.5N_2H_4$ nanobelts, (b) 1 at%, (c) 2 at%, (d) 3 at%, (e) 4 at%, and (f) 5 at%. The insets correspond to their optical images, respectively.

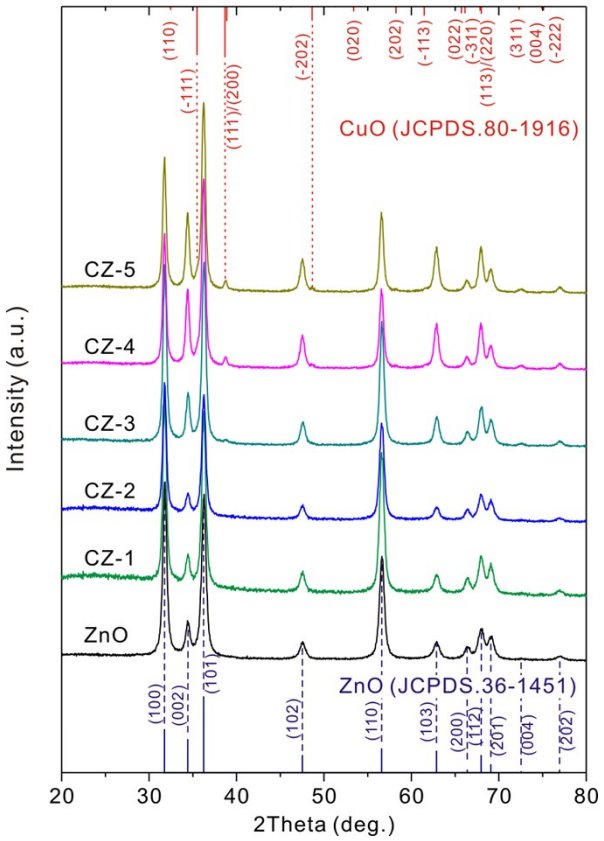

Figure S2. XRD patterns of as-prepared porous ZnO nanobelts doped with different concentrations of CuO.

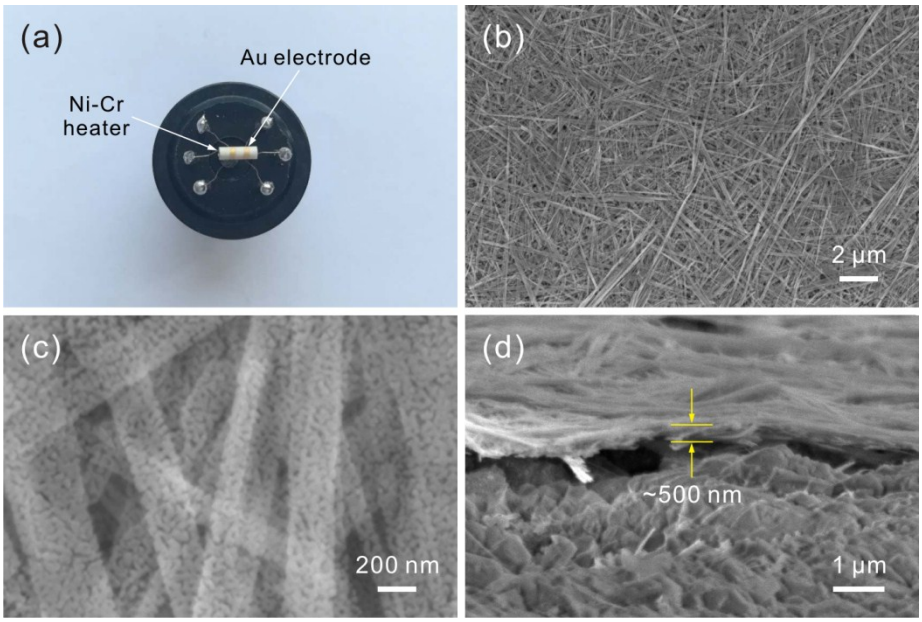

Figure S3. (a) Optical image of the fabricated sensing device, (b) low-magnification SEM image of top view of the sensing film and (c) its high-magnification SEM image, and (d) SEM image of cross section of the assembled sensing film.

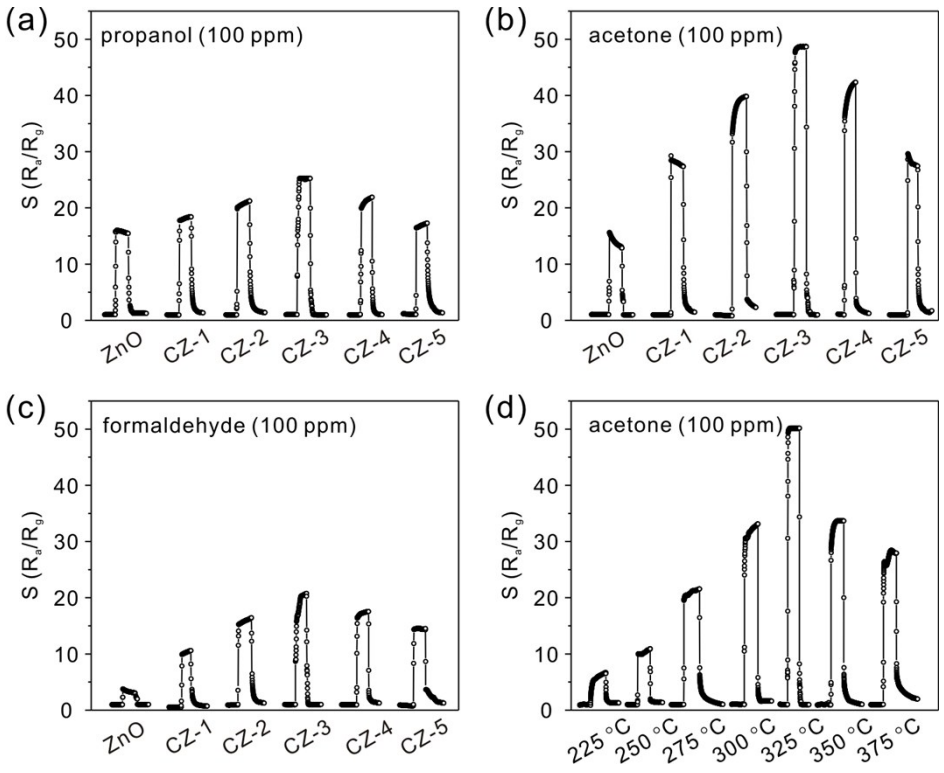

Figure S4. The relative response curves of different concentrations CuO-doped porous ZnO nanobelts toward 100 ppm of different typical VOCs: (a) propanol, (b) acetone and (c) formaldehyde at the working temperature of 325 ˚C, and (d) the relative response curves of CZ-3 porous nanobelts to 100 ppm acetone at different operating temperatures.

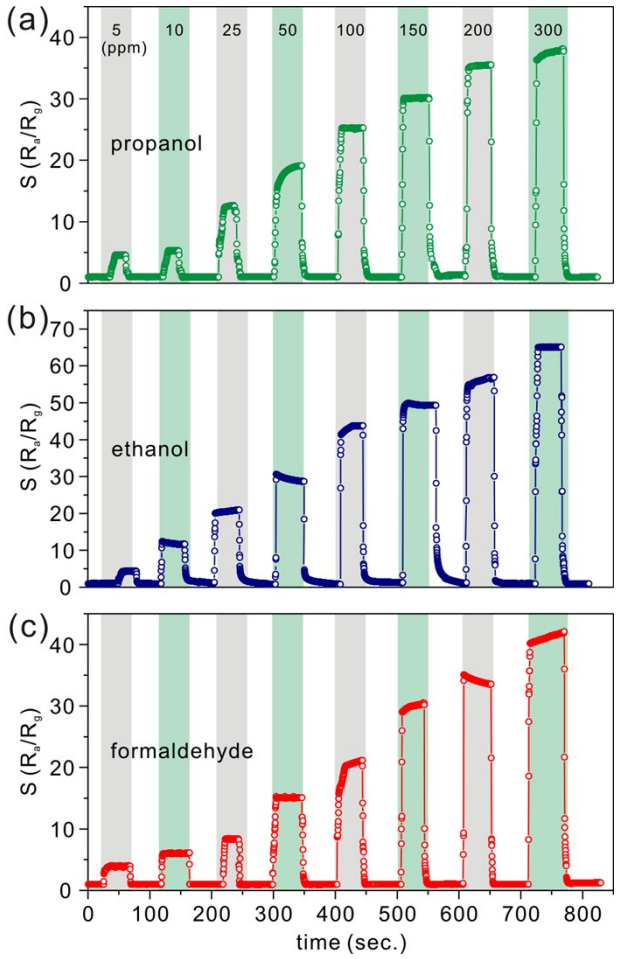

Figure S5. Real-time relative response curves of CZ-3 porous nanobelts toward different concentrations of propanol (a), ethanol (b) and formaldehyde (c) at the optimal working temperature of 325 ˚C.

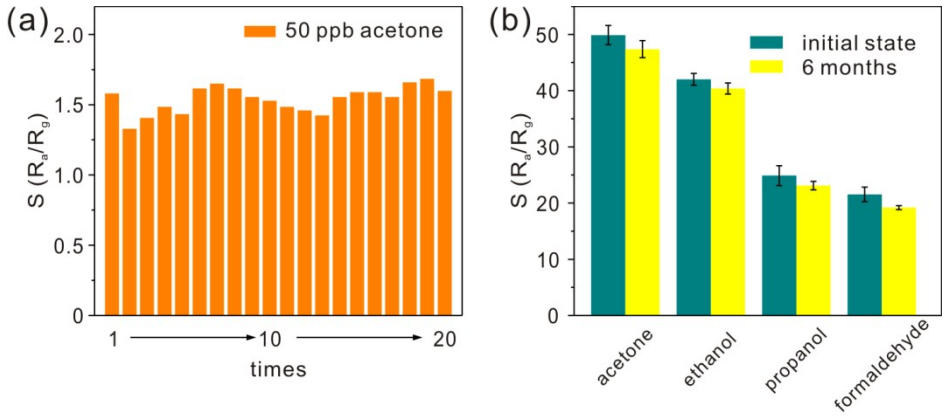

Figure S6. (a) the relative response of CZ-3 toward 50 ppb acetone for 20-cycle times and (b) the relative responses of porous CuO-doped ZnO nanobelts toward 100 ppm of acetone, ethanol, propanol and formaldehyde at the optimal working temperature of 325 °C before and after 6 about months.

Table S1. Theoretical and experimental concentration of the doped Cu (at %) for the porous CuO-doped ZnO nanobelts.

Sample	CZ-1	CZ-2	CZ-3	CZ-4	CZ-5
Theoretical concentration of Cu (at %)	1	2	3	4	5
Experimental concentration of Cu (at %)	1.19	2.22	3.29	4.26	5.16

Table S2. Comparison of the sensing properties of various acetone sensors based on CuO/ZnO.

Sample	Working Temperature (°C)	τ_{res}/τ_{rec}[a] (s)	Acetone Concentration (ppm)	S (R_a/R_g)	Refs
ZnO microsphere	330	11/17	100	22	[1]
Au/ZnO flowers	280	15/2	100	18.8	[2]
Co/ZnO nanofibers	360	6/4	100	4	[3]
Ni/SnO_2 nanofibers	340	-/-	100	3.8	[4]
Cu/ZnO/GO	340	15/15	10	9.4	[5]
Cu/ZnO flowers	220	-/-	10	7	[6]
CuO-doped porous ZnO nanobelts	**325**	**6/4**	**100/10**	**50/14**	**this work**

[a]τ_{res}: response time; τ_{rec}: recovery time.

[1] M. Y. Ge, T. M. Xuan, G. L. Yin, J. Lu, D. N. He, *Sens. Actuators, B* **2015**, 220, 356.

[2] Y. Lin, W. Wei, Y. Wang, J. R. Zhou, D. M. Sun, X. D. Zhang, S. P. Ruan, *J. Alloy Compd.* **2015**, 650, 37.

[3] L. Liu, S. C. Li, J. Zhuang, L. Y. Wang, J. B. Zhang, H. Y. Li, Z. Liu, Y. Han, X. X. Jiang, P. Zhang, *Sens. Actuators, B* **2011**, 155, 782.

[4] J. P. Cheng, B. B. Wang, M. G. Zhao, F. Liu, X. B. Zhang, *Sens. Actuators, B* **2014**, 190, 78.

[5] C. Wang, J. W. Zhu, S. M. Liang, H. P. Bi, Q. F. Han, X. H. Liu, X. Wang, *J. Mater. Chem. A* **2014**, 2, 18635.

[6] J. R. Huang, Y. J. Dai, C. P. Gu, Y. F. Sun, J. H. Liu, *J. Alloy Compd.* **2013**, 575, 115.